Macrophage Polarization Modulates Gene Expression Based on Extracellular Matrix (ECM) Cues

By

PERLA FARES

A Dissertation submitted to the
Department of Mechanical Engineering
in partial fulfillment of the
requirements for the degree of
Master of Science in Engineering
at The University of Michigan – Dearborn
2025

Master's Thesis Committee:

Dr. Caymen Novak – Assistant Professor, Chair

Dr. Aditya Raghunandan – Assistant Professor

Dr. Mathumai Kanapathipillai – Associate Professor

DECLARATION

I hereby declare that this dissertation has been prepared by myself and has not been submitted for any other degree previously. Datasets presented in each figure have been generated by me unless otherwise stated in the figure legend.

Perla Fares

May 9th, 2025

ACKNOWLEDGMENTS

"To grow, seek out rooms where others are wiser, more experienced, and more accomplished than you. If you're always the smartest person in the room, you're limiting your potential."

While this idea is widely quoted, the most popular version —

"If you're the smartest person in the room, you're in the wrong room"

—was the best advice I ever received.

Similar to a cell that grows faster and better in a microenvironment surrounded by others, I realized I grow best when I'm around the right people. And throughout my academic journey, I have been blessed enough to be surrounded by wonderful leaders, mentors, and peers, who constantly pushed me to question, learn, and grow: my family, friends, advisor, and colleagues.

I would like to express my deepest gratitude to my advisor, Dr. Caymen Novak, whose belief in me and high expectations helped me reach further than I ever imagined. The lessons I learned from her throughout this dissertation extend far beyond its pages, I learned lessons I will carry with me always.

I would like to thank the Experience Plus office at the University of Michigan-Dearborn for funding our work through the EXP+ independent research grant, and their assistantships in research. I would also like to thank the Department of Mechanical Engineering at the University of Michigan-Dearborn for nurturing a great academic environment to grow in.

Table of Contents

DECLARATION…….…….. ii

ACKNOWLEDGMENTS…….…….…… iii

LIST OF TABLES…….…….……. v

LIST OF FIGURES…….……..…….. v

LIST OF ABBREVIATIONS…….…… v

ABSTRACT……...……. 1

GRAPHICAL ABSTRACT…….…….……...…… 1

1. INTRODUCTION…….……...…… 2

1.1. Background…… 3

1.2. Motivation……..…… 5

1.3. Objective……..….. 5

2. METHODOLOGY…….…….…… 5

3. RESULTS…….……..…… 7

4. DISCUSSION……...…… 11

5. CONCLUSION……. 12

6. FUTURE DIRECTIONS……...…… 12

7. REFERENCES ……..…… 13

8. SUPPLEMENTARY MATERIAL……..…… 16

LIST OF TABLES

Table 1: Literature review

LIST OF FIGURES

Figure 1: UC experimental design
Figure 1b: qPCR analysis of UC cells
Figure 1c: UC Fold change summary
Figure 2: M1 experimental design
Figure 2b: qPCR analysis of M1-primed cells
Figure 2c: M1 Fold change summary
Figure 3: M2 experimental design
Figure 3b: qPCR analysis of M2-primed cells
Figure 3c: M2 Fold change summary

SUPPLEMENTARY MATERIALS

Table S1: qPCR primers
Figure S1: Bronchoalveolar lavage schematic overview
Figure S2: Recovery rates from AMs in 2D and 3D cultures

LIST OF ABBREVIATIONS

2D- Two-Dimensional

3D- Three-Dimensional

AM- Alveolar Macrophage

BAL- Bronchoalveolar lavage

CO_2- Carbon dioxide

CCL-17- C-C motif chemokine ligand 17

CCL-22 C-C motif chemokine ligand 22

cDNA- Complementary deoxyribonucleic acid

DMEM- Dulbecco's modified eagle's medium

DMSO- Dimethyl sulfoxide

F- Forward

FBS- Fetal bovine seru

H_2O- Water

ECM- Extracellular Matrix

ELISA- Enzyme-Linked Immunosorbent Assay

IL-1β- Interleukin 1-beta

IL-6- Interleukin 6

IL-10- Interleukin 10

IL-12- Interleukin 12

IL-23- Interleukin 23

IPF- Idiopathic Pulmonary Fibrosis

LPS- Lipopolysaccharide

M1 macrophage- Classically activated macrophage

M2 macrophage- Alternatively activated macrophage

mL- milliliters

mRNA- Messenger ribonucleic acid

NaOH- Sodium hydroxide

NOS-1- Neuronal nitric oxide synthase 1

PBS- Phosphate buffered saline

qPCR- Quantitative polymerase chain reaction

R- Reverse

RBC- Red blood cell

TGF-β- Transforming growth factor-beta

TNF-α- Tumor necrosis factor-alpha

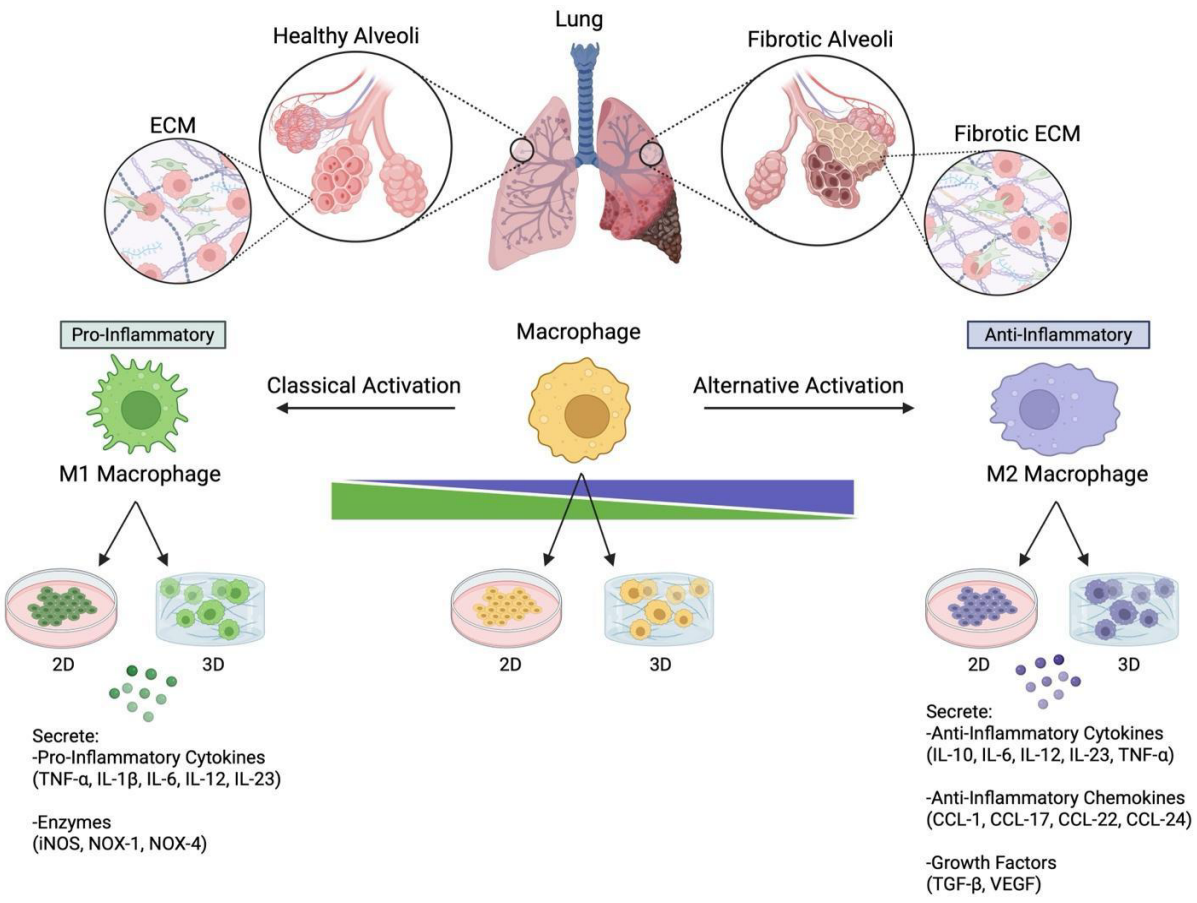
VEGF- Vascular endothelial growth factor

ºC- Degrees Celsius

ABSTRACT

Idiopathic pulmonary fibrosis (IPF) is a fatal lung disease characterized by excessive extracellular matrix (ECM) deposition, which stiffens the lung tissue and disrupts normal lung function. This increased mechanical activity dramatically alters the microenvironment. Within this environment, alveolar macrophages (AMs), the primary immune cells in the lung, play a central role in wound healing by shifting between pro-inflammatory M1 and pro-fibrotic M2 phenotypes. However, how the ECM or physical microenvironment influences AM polarization remains poorly understood. We hypothesize that these environmental changes, particularly matrix stiffness, can shape macrophage behavior. While 2D cultures are commonly used due to ease and accessibility, 3D cultures more closely mimic physiological lung conditions. In our study, we aim to create both 2D and 3D culture systems to: (1) determine whether the microenvironment is sufficient to drive macrophage polarization, and (2) assess whether prior polarization affects macrophage responses to different culture environments. By analyzing gene expression changes in 2D vs 3D cultures following no priming, M1 and M2 priming, our findings will clarify how ECM mechanics influence AM function, offering new insight into the wound healing process and fibrosis progression.

GRAPHICAL ABSTRACT



1. INTRODUCTION

Pulmonary fibrosis is a lung disease characterized by the scarring of lung tissue, causing difficulties in breathing [1]. Upon injury, different kinds of cells are recruited to the injury site with specific roles. Such cells include platelets, which aggregate to form clots, and consequently, activate various immune cells, such as monocytes and neutrophils, that release cytokines and other inflammatory mediators to initiate and regulate the healing response [2]. Following tissue injury, circulating monocytes differentiate into macrophages, adopting either a pro-inflammatory M1 phenotype or an anti-inflammatory M2 phenotype [3]. Initially, M1 macrophages are recruited to the injury site, where they release pro-inflammatory cytokines and growth factors and help clear cellular debris [3]. As inflammation resolves, M2 macrophages are recruited to promote tissue repair. They secrete anti-inflammatory mediators and stimulate fibroblasts, which then synthesize and deposit extracellular matrix (ECM) components, leading to the formation of a stiffer microenvironment [3]. The extracellular matrix (ECM) is a dynamic structure that surrounds cells and provides essential physical support and biochemical cues to maintain tissue organization and function. In idiopathic pulmonary fibrosis (IPF), fibroblasts are persistently activated and recruited to sites of injury, leading to excessive deposition of ECM proteins such as collagen. The increased ECM accumulation causes the lung tissue to stiffen, reducing its elasticity and impairing gas exchange, which results in difficulty breathing [1][4][5]. This alteration in the lung ECM plays a significant role in cellular responses and phenotypes [6]. ECM attributes contribute to cell behavior in both health and disease by providing signaling and structural cues to cells [7]. Serving as a reservoir for growth factors, and cytokines, and multiple cell types, the ECM is highly engaged in promoting the migration of distinct cell types to infected areas as part of the innate immune response [8].

Alveolar macrophages (AMs) are the main innate immune cells in the lung microenvironment responsible for maintaining lung homeostasis. AMs reside on the alveoli of the lungs, exposing them directly to external toxins like pollutants, pathogens, and dust. As key components of the lung's immune system, they act as frontline defenders, crucial for both initiating and resolving immune reactions. Consequently, alveolar macrophages play crucial roles in the lung microenvironment and are influenced by all aspects of the ECM. Rather than existing as a single functional population, AMs exhibit a broad spectrum of activation states, ranging from pro-inflammatory to pro-fibrotic phenotypes, which allows them to regulate immune responses to the lung's changing environment [6][9][10]. AM polarization phenotypes are dictated by external stimuli [8]. Macrophages are commonly classified as classically activated (M1), or alternatively activated (M2) cells, where the M1 Phenotype is induced by infection and pro-inflammatory cytokines, such as LPS, IL-1ß, IL-6, IL-12, and TNFα [8][11]. In contrast, M2 phenotypes are induced by anti-inflammatory cytokines, such as IL-4, IL-10, IL-13 and TGF-β [8][11].

AMs play a major role in the progression of fibrosis. During the early phase, M1 macrophages secrete pro-fibrotic cytokines that activate fibroblasts and drive their differentiation into ECM-producing myofibroblasts. As cytokine levels rise, a proportionally larger population of fibroblasts undergoes this transition, leading to enhanced ECM deposition and fibrosis progression [7][10]. In contrast, the later-phase M2 macrophages are activated for remodeling purposes, and although not fully understood, Wight et al (2017) proposes that M2 macrophages may play a

crucial role in fibrosis resolution [8]. Macrophages can be polarized through treatment with specific skewing agents that drive M1 (like lipopolysaccharide, or LPS) and M2 phenotypes (such as interleukin-4, IL-4, and interleukin-13, IL-13) [12].

Macrophages can polarize into distinct phenotypes depending on environmental cues, a process guided by specific skewing agents. Exposure to LPS, a bacterial component, triggers TLR4 signaling and promotes an M1-like phenotype characterized by pro-inflammatory cytokine production and pathogen defense. In contrast, IL-4 and IL-13 activate the STAT6 pathway via IL-4Rα, driving macrophages toward an M2-like phenotype associated with wound healing, tissue repair, and fibrosis [9][13].

Recent studies have explored how ECM stiffness and culture dimensionality influence macrophage polarization [14]. While some studies associated stiffer environments with an M1 phenotypic behavior, others have found the exact opposite, reporting that increased matrix stiffness can instead promote an M2-like phenotype [15]. These discrepancies likely arise from differences in how the microenvironments were defined, including variations in matrix stiffness, culture dimensionality (2D vs. 3D), priming durations, cell types used, and overall experimental design [16].

To parse these contrasting findings, the following studies show how macrophage polarization varies across different stiffness levels and culture environments. Previtera and Sengupta cultured mouse bone marrow–derived macrophages (BMDMs) on polyacrylamide gels of varying stiffness (0.3–230 kPa) and observed that stiffer substrates enhanced proinflammatory mediator production through TLR4 activity, indicating a shift toward the M1 phenotype [17]. Chakraborty et al. used human monocyte-derived macrophages on soft (0.1 kPa) and stiff (10.3 kPa) PEG hydrogels, finding that softer substrates maintained M2 polarization, while stiffer ones promoted M1 markers [18]. Sridharan et al. examined THP-1-derived macrophages on substrates with stiffness ranging from 11 to 323 kPa, noting that increased stiffness favored M1 polarization, as evidenced by elevated proinflammatory cytokines [11]. Luo et al. demonstrated that matrix stiffening activates the Piezo1–YAP signaling axis in BMDMs, leading to M1 polarization and altered immunometabolism [19]. Patel et al. highlighted that macrophage elasticity, influenced by substrate stiffness, determines innate immune function across different macrophage types [20]. Helleberg Madsen et al. compared 2D and 3D cancer models, revealing that 3D cultures better mimic in vivo conditions and affect macrophage polarization differently than 2D cultures [21]. Mas-Rosario et al. developed an iNOS reporter to study macrophage polarization in 2D and 3D breast cancer models, finding that 3D environments influence macrophage reprogramming [22]. Carrara et al. showed that 3D topographies promote differentiation into the anti-inflammatory M2d subset, with increased IL-10 secretion [23]. Tiemeijer et al. utilized thermo-reversible hydrogels in droplet-based microfluidics to assess single-cell macrophage polarization, highlighting the impact of 3D culture on macrophage heterogeneity [24]. Graf et al. cultured RAW 264.7 cells, IC-21 cells, and primary macrophages (peritoneal and bone marrow–derived) in both 2D plastic and 3D hydrogel environments to

evaluate how macrophage origin and culture dimensionality influence polarization. They found that macrophage behavior varied depending on cell source, with primary and immortalized lines responding differently to environmental cues. Notably, cells cultured in 3D hydrogels exhibited reduced polarization compared to those in 2D, highlighting the suppressing effect of physiologically soft environments on macrophage activation [25].

Table 1: Summary of studies that assessed macrophage polarization in different cell types, microenvironment cultures, priming conditions, and durations.

Article Details	Cell/ Tissue Type	Substrate Stiffness	Priming Condition	Duration	Key Findings
Previetera et al., *Bioactive Materials*, 2021	Mouse bone marrow–derived macrophages (BMMs)	~2.5 kPa (low), ~35 kPa (medium), ~63 kPa(high)	None (no cytokines added)	5 days	Stiff = M2
Chakraborty et al., *Acta Biomaterialia*, 2021	Human cord blood monocyte–derived macrophages ($CD14^+$ cells)	0.1, 3.4, 10.3 kPa (PEG hydrogels)	LPS + IFN-γ (M1); IL-4 + IL-13 (M2a); IL-10 (M2c)	3 days	Stiff = M2
Sridharan et al., *Acta Biomaterialia*, 2019	THP-1 monocytes PMA-differentiated to macrophages	11 kPa (soft), 88 kPa (medium), 323 kPa (stiff)	None (no polarizing cytokines)	~24 h	Stiff = M1, Soft = M2
Luo et al., *Clinical and Translational Medicine*, 2022	Mouse bone marrow–derived macrophages (BMDMs)	11 kPa (soft), 88 kPa (medium), 323 kPa (stiff)	None (no polarizing cytokines)	~24 h	Stiff = M1, Soft = M2
Patel et al., *PLoS ONE*, 2016	Mouse BMDMs	0.3 kPa (soft) vs 230 kPa (stiff)	LPS (M1 stimulation); no M2 condition	24 h	Stiff = M1
Helleberg Madsen et al., *Cell. Immunol.*, 2022	Human monocyte-derived macrophages	2D: plastic; 3D: tumor spheroid co-culture	Co-cultured with tumor cells; drugs (CD40L, CSF-1Ri)	3–5 days	3D = M2
Mas-Rosario et al., *Front. Oncol.*, 2023	RAW 264.7 iNOS-GFP reporter line	2D: plastic; 3D: tumor spheroids	Tumor co-culture ± small molecule(PBI1)	48 h	3D = M2
Carrara et al., *Mater. Today, Bio*, 2024	THP-1–derived macrophages	2D: flat glass; 3D: fractal topographical surface	None (spontaneous polarization)	3 days	3D = M2

Tiemeijer et al., *Front. Bioeng. Biotechnol.*, 2021	Human primary monocyte–derived macrophages	2D: droplet suspension; 3D: hydrogel droplet (~100 Pa)	± IL-4/IL-13	24 h	3D = M2
Graf et al., *Front. Biomater. Sci.*, 2024	RAW 264.7, IC-21, primary peritoneal & BMDMs	2D: stiff plastic; 3D: soft hydrogel (~100–200 Pa)	LPS, IL-4, IL-13	24–48 h	M2 ↓ in 3D

Given the extensive contradictions reported in the literature, there remains limited understanding of how the physical microenvironment influences macrophage polarization and their response after priming. To help resolve the problem, we developed a culture system that allows us to assess macrophage polarization with the following objectives:

1. Determine whether the microenvironment is sufficient to drive macrophage polarization.
2. Evaluate whether polarization can influence response to 3D culture environments.

Since IPF is a mechanically driven disease that alters the tissue microenvironment, we hypothesize that these changes in the microenvironment can affect macrophage polarization. To test this hypothesis, we used 2D and 3D hydrogel-based culture systems to assess how the microenvironment influenced macrophage behavior following polarization.

2. METHODOLOGY

2.1 Cell culture

RAW 264.7 cells, purchased from the American Type Culture Collection (ATCC, TIB-71), were obtained through donation from Dr. Kalyan Kodnapalli at the University of Michigan-Dearborn. To sustain cell culture, the cells were maintained in Dulbecco's Modified Eagle's Medium (DMEM, #11965092, ThermoFisher Scientific), supplied with 10% fetal bovine serum (FBS, #FB12999102, ThermoFisher Scientific), and 5% antibiotic-antimycotic solution (#15240062, Gibco). Cells were cultured under 5% CO_2 at 37 ºC and passaged at 75% confluency.

For 3D cultures, RAW 264.7 cells were encapsulated in 21 mg/mL type I bovine collagen hydrogel (#103700-658, VWR). All reagents were kept on ice throughout the procedure. A master mix was prepared by combining water, 10x PBS (#14040133, Gibco) with phenol red, and 1M NaOH to a final pH ~7.4. Then, collagen was added slowly to prevent bubble formation. The mixture was gently pipetted until homogeneous. Next, 500 µL of cell suspension, at a 2×10^6 cells/mL concentration, was added to each collagen mix and mixed gently. The total mixture was then transferred to a 12-well plate and incubated at 37°C for 45 minutes to allow gelation. After crosslinking, gels were transferred to culture-treated 6-well plates (07-200-83, Fisher Scientific) pre-filled with 3 mL of warm culture medium.

2.2 Gene expression quantification

2.2.1 Sample Preparation

Cells were cultured into 2D tissue culture plates and treated with 50 ng/mL of lipopolysaccharide (LPS) (M1 priming) and 50 ng/mL of both IL-4 and 50 ng/mL of IL-13 for 24 hours (M2 priming) [19]. Then, cells were passaged into 2D and 3D environments and incubated for another 24 hours. Cells were then collected and lysed for gene expression analysis. All experiments were conducted using cells between passages 19 and 24.

2.2.2 mRNA extraction

Messenger RNA (mRNA) was isolated from RAW 246.7 using the Aurum total RNA mini kit (#7326820, BioRad) following the manufacturer's instructions. The 3D hydrogel cultures were resuspended in the kit's lysate buffer. Extracted mRNA concentration was measured using Nanodrop one spectrophotometer (#13-400-525, ThermoFisher Scientific) to measure the amount and purity of the mRNA. The ideal RNA concentration was expected to range between 100 –1000 ng/µL. For purity assessment, A260/A280 and A260/A230 ratios were evaluated to be as close as possible to 2.0.

2.2.3 cDNA synthesis

Complementary DNA (cDNA) was synthesized from 750 ng of extracted mRNA using the iScript cDNA synthesis kit (#1708890, BioRad), according to the manufacturer's instructions. Briefly, mRNA was diluted in nuclease-free water and added to 1-part of the iScript reverse transcriptase and 4 parts of the 5x iScript reaction mix, then incubated in a thermal cycler.

2.2.4 Pig qPCR primer design

After identifying *Sus scrofa* as the scientific name of the pig organism, the genes of interest were looked up on the National Library of Medicine-National Center for biotechnology information website, under "gene". The NCBI RefSeq mRNA accession number (NM number) and NCBI RefSeq accession number (XM number) for mRNA and proteins were then found and exported into the qPCR primer database and searched for under "organism". A list of relevant gene sequences was generated, and the final target sequence was selected based on the following criteria: short nucleotide length, approximately 50% GC content, presence of a GC clamp, and a melting temperature (Tm) between 55–65 °C with less than a 1 °C difference between forward and reverse primers [26]. The selected sequence was then verified for specificity using NCBI BLAST to ensure accurate alignment with the gene of interest [27] (Table S1).

2.2.5 Gene expression quantification by qPCR

Quantitative real time PCR analysis experiments were set up using the Sybr Green Master Mix (Applied systems, ThermoFisher) according to the manufacturer's instructions and ran on the CFX Opus real time PCR machine (Biorad). Cycle threshold (Ct) values were first normalized to

controls and used to calculate the relative normalized fold change [28]. To account for variability, assays were performed in three biological replicates with three technical replicates each. Primer sequences used for both mouse and pig are listed (Table S1).

2.3 Alveolar macrophage isolation

Red cross waddle pig lungs were obtained from Scholl's slaughterhouse (Blissfield, MI). The lung lobes were separated by carefully cutting them apart with sterile scissors. A funnel was inserted into the main bronchi leading to the interior of the diaphragmic lobe and sterile 1xPBS was poured in to rinse out the inside of the alveoli and recover the AMs. The lobe was then gently massaged. AMs were collected by transferring the PBS solution into a tube and centrifuging it to pellet the cells. Red blood cells were removed using sterile H_2O, vortexed for 20-30s, followed by neutralization with media and a second centrifugation. The resulting pellet was then washed with PBS to obtain purified AMs. AMs were quantified, tested for viability, and cryopreserved at 5 million cells per mL in cryovials containing 10% DMSO (#BP231-1, ThermoFisher) in 90% FBS. Samples were stored at –80 °C for further analyses (Fig. S1). Preliminary data supporting AM isolation and viability validation are shown in Supplemental Figure S2.

3. RESULTS

3.1 3D culture microenvironment upregulates gene expression in RAW 264.7 cells.

To investigate whether the microenvironment is sufficient to drive macrophage polarization, we cultured RAW 264.7 macrophages then passaged them into 2D culture plates and 3D collagen hydrogel matrices for 24 hrs. Cells were collected and analyzed for gene expression changes with qPCR. All gene expression data were normalized to cells cultured under 3D conditions, allowing direct comparison of microenvironment-driven effects on macrophage polarization. To assess macrophage polarization, we used pro-inflammatory cytokines (M1-associated makers) IL-23, NOS-1, IL-1β, IL-6, and TNF-α, to quantify M1-like phenotype. These genes are expected to increase in M1 polarized macrophages [13]. Gene expression changes of anti-inflammatory cytokines (M2-associated markers) were also quantified to assess M2-like phenotypic changes. The M2-associated markers used were VEGF, CCL-22, TGF-β, and IL-10, and were expected to increase in M2 polarized macrophages [13]. Our results show that when RAW cells are cultured in 3D microenvironments, the gene expression of most M1-associated markers (including IL-23 and NOS-1) except for IL-1β, was increased. This trend persevered in M2-associated markers as their gene expression was also significantly upregulated (VEGF, CCL-22, and TGF-β). Although not biologically significant, some other genes showed a downregulation (IL-6, TNF-α, and IL-10) (Fig. 1).

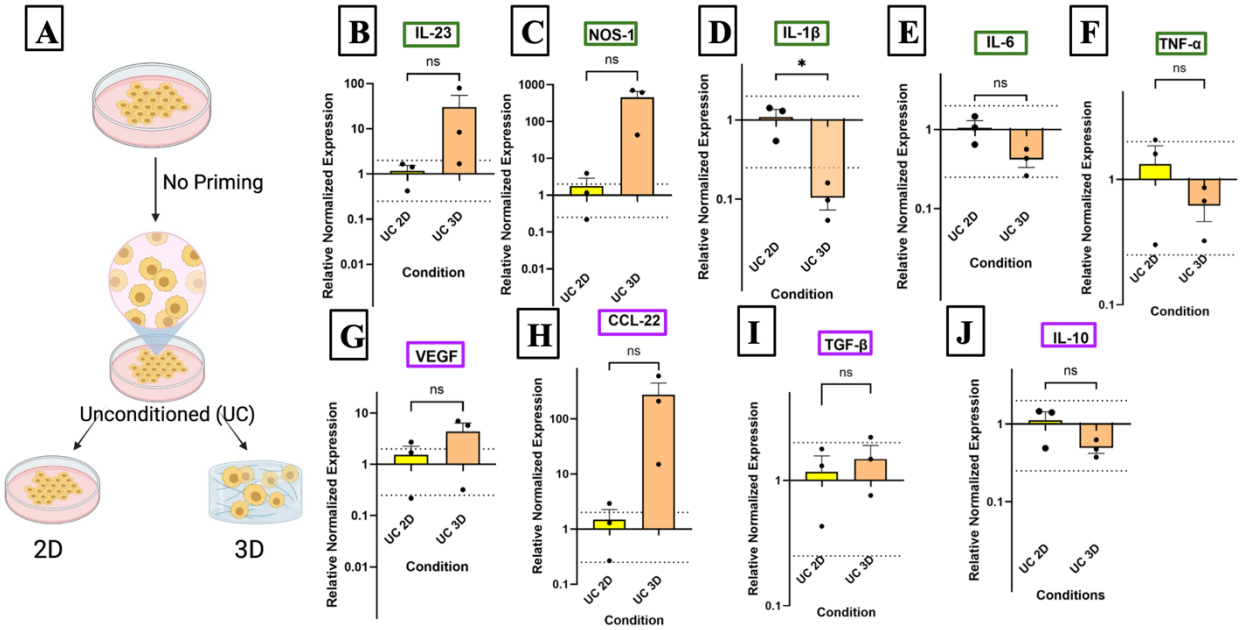


Figure 1. Gene expression analysis of unconditioned cells in 2D and 3D microenvironments. (A) Schematic overview showing the culture of RAW 264.7 cells without priming agents to maintain an UC phenotype. Cultured cells were then passaged in either 2D tissue culture plates or encapsulated in 3D collagen hydrogels for downstream analysis of gene expression. Relative normalized gene expression analysis of unconditioned RAW 264.7 cells cultured in 2D versus 3D microenvironments. Gene expression analysis of M1-associated markers (B) IL-23, (C) NOS-1, (D) IL-1β, (E) IL-6, and (F) TNF- α, as assessed via qPCR. Gene expression analysis of M2-associated markers (G) VEGF, (H) CCL-22, (I) TGF- β, and (J) IL-10, as assessed via qPCR. Error bars represent standard error of mean (SEM) of three biological replicates with three technical replicates each. Statistical analysis was performed using unpaired t-tests; *$p < 0.05$, ns = not significant. Dotted lines represent thresholds for biologically significant gene expression changes, with the upper line indicating upregulation and the lower line indicating downregulation. Biological significance is defined as a gene expression change showing at least a two-fold increase (upregulation) or a two-fold decrease (downregulation). Data variability among replicates resulted in non-significant statistical differences. Hence, unprimed RAW 264.7 macrophages show a minor upregulation in gene expression changes when cultured in 3D microenvironments.

3.2 3D culture microenvironment upregulates gene expression in M1-primed RAW 264.7 macrophages

To investigate whether prior polarization affects macrophage responses to different culture environments, we cultured RAW 264.7 macrophages, treated them with LPS to polarize the cells to M1 macrophages, and then passaged them into 2D culture plates and 3D collagen hydrogel matrices for 24 hrs. Cells were collected and analyzed for gene expression changes with qPCR. All gene expression data were normalized to cells cultured under 3D conditions, allowing direct comparison of microenvironment-driven effects on macrophage polarization. To assess

macrophage polarization, we quantified pro-inflammatory cytokines (M1-associated makers) and anti-inflammatory cytokines (M2-associated markers) (previously described). M1-associated markers are expected to increase in M1 polarized macrophages and M2-associated markers are expected to increase in M2 polarized macrophages. Our results show that when RAW cells are cultured in 3D microenvironments after M1-priming, the gene expression of all M1-associated markers was increased (NOS-1, TNF-α, IL-6, IL-23, and IL-1β). The trend persevered in all M2-associated markers as their gene expression was also significantly upregulated (IL-10, CCL-22, TGF-β, VEGF) (Fig. 2).

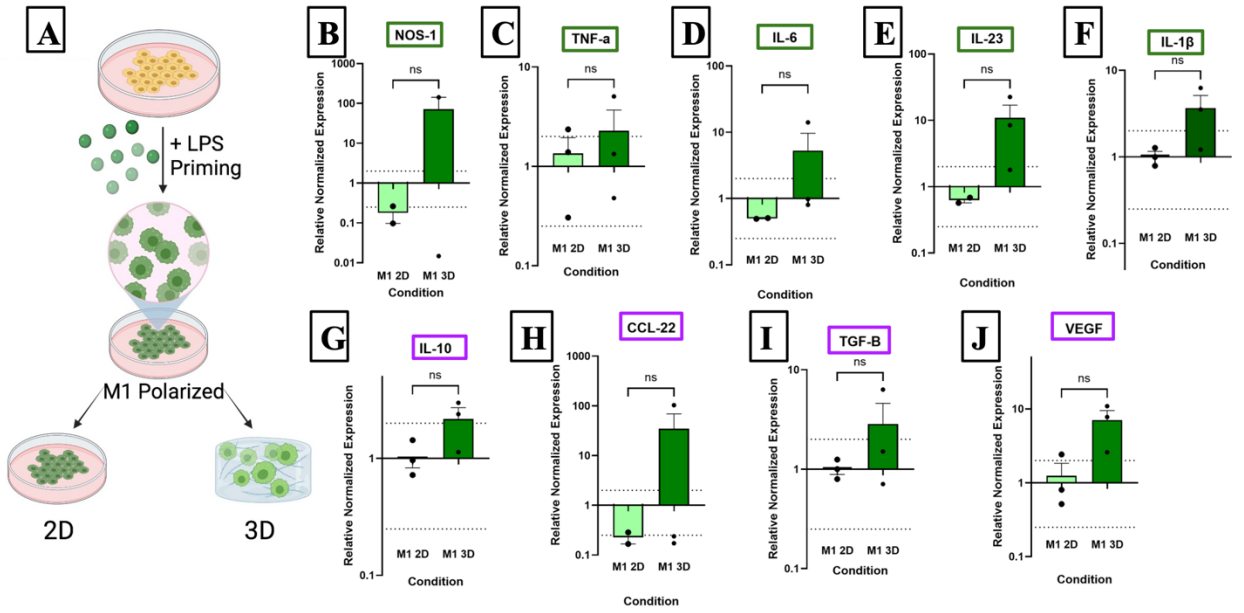


Figure 2: Gene expression analysis of M1-primed cells in 2D and 3D microenvironments. (A) Schematic overview showing the culture of RAW 264.7 cells with LPS priming agent, for an M1 polarization. Cells were then passaged in either 2D tissue culture plates or encapsulated in 3D collagen hydrogels for downstream analysis of gene expression. Relative normalized gene expression analysis of M1-primed RAW 264.7 cells cultured in 2D versus 3D microenvironments. Gene expression analysis of M1-associated markers (B) NOS-1, (C) TNF- α, (D) IL-6 β, (E) IL-23, and (F) IL-1 β, as assessed via qPCR. Gene expression analysis of M2-associated markers (G) IL-10, (H) CCL-22, (I) TGF- β, and (J) VEGF, as assessed via qPCR. Error bars represent standard error of mean (SEM) of three biological replicates with three technical replicates each. Statistical analysis was performed using unpaired t-tests; ns = not significant. Dotted lines represent thresholds for biologically significant gene expression changes, with the upper line indicating upregulation and the lower line indicating downregulation. Biological significance is defined as a gene expression change showing at least a two-fold increase (upregulation) or a two-fold decrease (downregulation). Data variability among replicates resulted in non-significant statistical differences. Hence, M1-primed RAW 264.7 macrophages show an upregulation in gene expression changes in 3D culture compared to 2D culture microenvironments.

3.2 3D culture microenvironment downregulates gene expression in M2-primed RAW 264.7 macrophages

To investigate how M2 polarization affects cellular responses to 3D culture environments, we cultured RAW 264.7 macrophages, treated them with IL-4/IL-13 to polarize the cells to M2 macrophages, then passaged them into 2D culture plates and 3D collagen hydrogel matrices for 24 hrs. Cells were collected and analyzed for gene expression changes with qPCR. All gene expression data were normalized to cells cultured under 3D conditions, allowing direct comparison of microenvironment-driven effects on macrophage polarization. To assess macrophage polarization, we quantified pro-inflammatory cytokines (M1-associated makers) and anti-inflammatory cytokines (M2-associated markers) (as previously described). Our results show that when RAW cells are cultured in 3D microenvironments after M2-priming, the gene expression of most M1-associated markers, except for TNF-α was significantly downregulated (IL-1β, IL-6, IL-23, and NOS-1). TNF-α was the only M1-associated gene that showed a biologically significant upregulation when cultured in 3D following M2 priming. The trend persevered in all M2-associated markers as their gene expression was also significantly downregulated (TGF-β, CCL-22, and VEGF). There were no significant gene expression changes observed for IL-10 (Fig. 3).

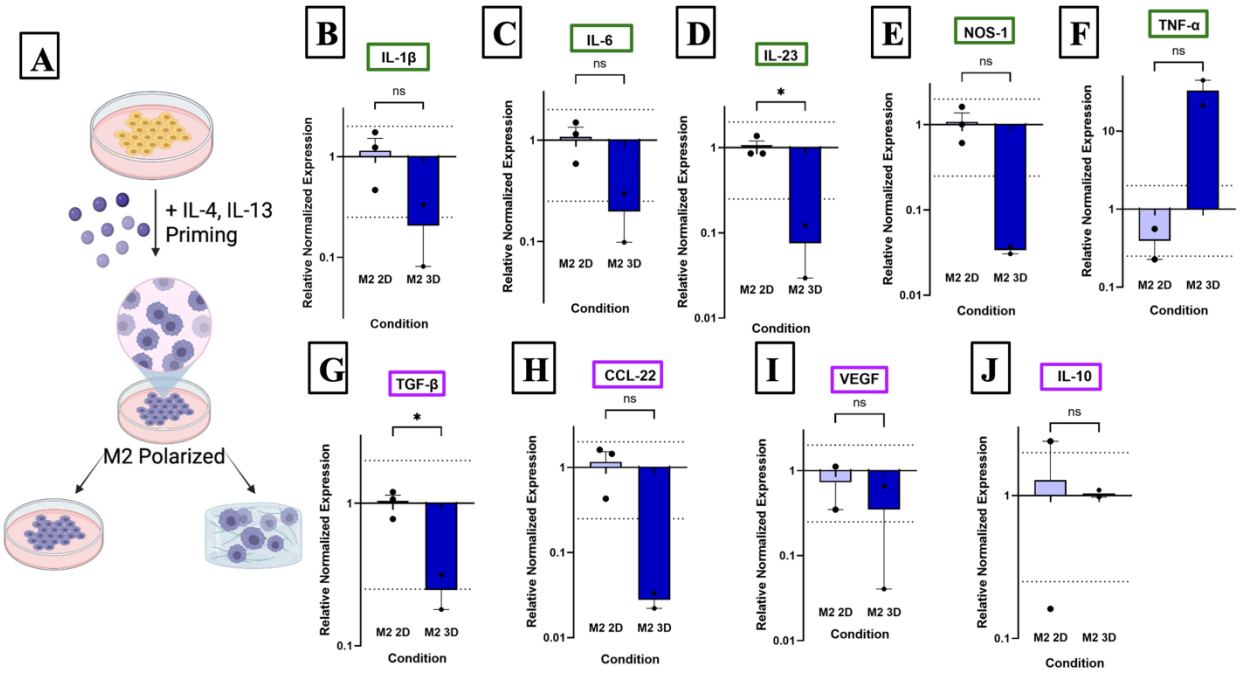


Figure 3: Gene expression analysis of M1-primed cells in 2D and 3D microenvironments. (A) Schematic overview showing the culture of RAW 264.7 cells with IL-4, IL-13 priming agent, for an M2 polarization. Cells were then passaged in either 2D tissue culture plates or encapsulated in 3D collagen hydrogels for downstream analysis of gene expression. Normalized gene expression analysis of M2-primed RAW 264.7 cells cultured in 2D versus 3D microenvironments. Gene expression analysis of M1-associated markers (B) IL-6 β, (C) IL-6, (D) IL-23 β, (E) NOS-1, and (F) TNF- α as assessed via qPCR. Gene expression analysis of M2-associated markers (G) TGF-

β, (H) CCL-22, (I) VEGF, and (J) IL-10, as assessed via qPCR. Error bars represent standard error of mean (SEM) of three biological replicates with three technical replicates each. Statistical analysis was performed using unpaired t-tests; *$p < 0.05$, ns = not significant. Dotted lines represent thresholds for biologically significant gene expression changes, with the upper line indicating upregulation and the lower line indicating downregulation. Biological significance is defined as a gene expression change showing at least a two-fold increase (upregulation) or a two-fold decrease (downregulation). Data variability among replicates resulted in non-significant statistical differences. Hence, M2-primed RAW 264.7 macrophages show a downregulation in gene expression changes in 3D culture compared to 2D culture microenvironments.

4. DISCUSSION

Macrophages play a central role in the initiation, progression, and resolution of IPF, orchestrating inflammatory signaling, extracellular matrix remodeling, and tissue repair responses. To modulate macrophage activation states and better understand their role in fibrotic signaling, RAW 264.7 were treated in 3 different treatments: without pre-priming (UC), with M1-priming, and with M2-priming, then were passaged into 2D and 3D culture microenvironments and evaluated for downstream gene expression changes. Overall, in UC cells, the expression of several genes was significantly upregulated. M1-primed macrophages showed a significant upregulation in all genes when cultured in 3D, while, interestingly, M2-primed macrophages showed a significant downregulation in most genes when cultured in 3D. We did not observe a significant difference in gene expression levels between M1 and M2-associated genes within a condition.

More specifically, our data suggest that the extracellular matrix ECM significantly influences macrophage gene expression and polarization states, although it is not driving it towards a specific polarization phenotype. In unconditioned macrophages, 3D collagen hydrogels induced upregulation of several M2-associated genes (e.g., VEGF, CCL-22, IL-10), suggesting a bias toward an anti-inflammatory, reparative phenotype. This is consistent with prior findings indicating that softer or more physiologically relevant 3D environments encourage M2-like responses, supporting our interpretation that a 3D or softer ECM mimics a wound-healing environment, promoting anti-inflammatory signaling [27].

Interestingly, M1-primed macrophages cultured in 3D also showed significant increases in both M1 (IL-1β, IL-6, TNF-α) and M2 (IL-10) gene expression, implying that the 3D environment amplifies activation signals. This dual expression suggests phenotypic versatility in response to environmental cues, highlighting the importance of dimensionality in shaping immune behavior [15]. In contrast, M2-primed macrophages placed in 3D culture showed a general downregulation of both M1 and M2 markers, except for TNF-α, which was paradoxically elevated. Notably, such changes in macrophage behavior have been observed in prior work using decellularized fibrotic ECM and tumor models [20].

Collectively, our results support the conclusion that culturing macrophages in 3D microenvironment will play a role in regulating the gene expression changes of M1- and M2-associated markers. Depending on the priming context, macrophages will show either an upregulation or a downregulation in their gene expressions. This highlights the complexity of macrophage behavior in physiologically relevant settings. Notably, several comparisons did not reach statistical significance, likely due to high variability among biological replicates and a limited number of samples, which reduced statistical significance. Increasing the number of replicates, incorporating complementary assays, and validating findings in primary cells, in future studies would help minimize variance and strengthen the validity of these observations. Further studies are needed to determine whether this adaptability plays a protective or pathological role in disease contexts like fibrosis.

5. CONCLUSION

This study demonstrates that the 3D culture environment plays a role in shaping macrophage gene expression. For the specific genes that we have tested (NOS-1, TNF- α, IL-6 β, IL-23, IL-1β, IL-10, CCL-22, TGF- β, and VEGF), gene expression in unconditioned macrophages significantly increased in 3D culture environments. Gene expression in M1-primed macrophages showed a significant upregulation in 3D, while M2-primed cells showed the total opposite, with most genes significantly downregulated when cultured in 3D.

These findings highlight the importance of evaluating macrophage behavior in both 2D and 3D systems. While 2D culture is easier, faster, and more commonly used, 3D models offer a more physiologically relevant environment that better mimics in vivo conditions. This distinction is essential not only for accurately characterizing immune responses but also for advancing the development of therapeutic interventions. A deeper understanding of how macrophages behave within physiologically relevant in-vitro systems, particularly those that better mimic the complexity of the in-vivo microenvironment, is crucial for generating results that are predictive of patient outcomes and translatable to clinical care [29][30][31].

6. FUTURE DIRECTIONS

In the short term, work will focus on validating gene expression findings through protein expression analyses and quantification using ELISA, Western blotting, and flow cytometry. Additional efforts will include confirming these results in primary cells, specifically pig AMs, and conducting time-course experiments to assess the dynamics of cellular responses to their microenvironment under polarization over time.

In the long term, this study will expand to explore the behavior of AMs while being cultured on tissue-specific microenvironments, both diseased and healthy, and apply dynamic mechanical stimuli to better mimic physiological conditions. Finally, findings will be validated in human macrophages to ensure translational relevance.

7. REFERENCES

[1] V. J. Thannickal, G. B. Toews, E. S. White, J. P. Lynch Iii, and F. J. Martinez, "Mechanisms of Pulmonary Fibrosis," *Annu. Rev. Med.*, vol. 55, no. 1, pp. 395–417, Feb. 2004, doi: 10.1146/annurev.med.55.091902.103810.

[2] Y. Jiang *et al.*, "Macrophages in organ fibrosis: from pathogenesis to therapeutic targets," *Cell Death Discov.*, vol. 10, no. 1, p. 487, Dec. 2024, doi: 10.1038/s41420-024-02247-1.

[3] V. J. Thannickal *et al.*, "Matrix Biology of Idiopathic Pulmonary Fibrosis," *Am. J. Pathol.*, vol. 184, no. 6, pp. 1643–1651, June 2014, doi: 10.1016/j.ajpath.2014.02.003.

[4] P. J. Murray and T. A. Wynn, "Protective and pathogenic functions of macrophage subsets," *Nat. Rev. Immunol.*, vol. 11, no. 11, pp. 723–737, Nov. 2011, doi: 10.1038/nri3073.

[5] M. Friedemann *et al.*, "Instructing Human Macrophage Polarization by Stiffness and Glycosaminoglycan Functionalization in 3D Collagen Networks," *Adv. Healthc. Mater.*, vol. 6, no. 7, p. 1600967, Apr. 2017, doi: 10.1002/adhm.201600967.

[6] F. Y. McWhorter, C. T. Davis, and W. F. Liu, "Physical and mechanical regulation of macrophage phenotype and function," *Cell. Mol. Life Sci.*, vol. 72, no. 7, pp. 1303–1316, Apr. 2015, doi: 10.1007/s00018-014-1796-8.

[7] M. S. Wilson and T. A. Wynn, "Pulmonary fibrosis: pathogenesis, etiology and regulation," *Mucosal Immunol.*, vol. 2, no. 2, pp. 103–121, Mar. 2009, doi: 10.1038/mi.2008.85.

[8] V. J. Thannickal *et al.*, "Matrix Biology of Idiopathic Pulmonary Fibrosis," *Am. J. Pathol.*, vol. 184, no. 6, pp. 1643–1651, Jun. 2014, doi: 10.1016/j.ajpath.2014.02.003.

[9] J.-Q. Ban, L.-H. Ao, X. He, H. Zhao, and J. Li, "Advances in macrophage-myofibroblast transformation in fibrotic diseases," *Front. Immunol.*, vol. 15, p. 1461919, Oct. 2024, doi: 10.3389/fimmu.2024.1461919.

[10] J. He, X. Cheng, B. Fang, S. Shan, and Q. Li, "Mechanical stiffness promotes skin fibrosis via Piezo1-Wnt2/Wnt11-CCL24 positive feedback loop," *Cell Death Dis.*, vol. 15, no. 1, p. 84, Jan. 2024, doi: 10.1038/s41419-024-06466-3.

[11] E. S. White, "Lung Extracellular Matrix and Fibroblast Function," *Ann. Am. Thorac. Soc.*, vol. 12, no. Supplement 1, pp. S30–S33, Mar. 2015, doi: 10.1513/AnnalsATS.201406-240MG.

[12] T. N. Wight, C. W. Frevert, J. S. Debley, S. R. Reeves, W. C. Parks, and S. F. Ziegler, "Interplay of extracellular matrix and leukocytes in lung inflammation," *Cell. Immunol.*, vol. 312, pp. 1–14, Feb. 2017, doi: 10.1016/j.cellimm.2016.12.003.

[13] P. J. Murray and T. A. Wynn, "Protective and pathogenic functions of macrophage subsets," *Nat. Rev. Immunol.*, vol. 11, no. 11, pp. 723–737, Nov. 2011, doi: 10.1038/nri3073.

[14] T. Shi, L. Denney, H. An, L.-P. Ho, and Y. Zheng, "Alveolar and lung interstitial macrophages: Definitions, functions, and roles in lung fibrosis," *J. Leukoc. Biol.*, vol. 110, no. 1, pp. 107–114, Jun. 2021, doi: 10.1002/JLB.3RU0720-418R.

[15] J. Zeng, Y. Zhang, and C. Huang, "Macrophages polarization in renal inflammation and fibrosis animal models (Review)," *Mol. Med. Rep.*, vol. 29, no. 2, p. 29, Dec. 2023, doi: 10.3892/mmr.2023.13152.

[16] N. Wang, H. Liang, and K. Zen, "Molecular Mechanisms That Influence the Macrophage M1-M2 Polarization Balance," *Front. Immunol.*, vol. 5, Nov. 2014, doi: 10.3389/fimmu.2014.00614.

[17] Mantovani, A., et al. (2004). The chemokine system in diverse forms of macrophage activation and polarization. Trends in Immunology, 25(12), 677–686.

https://doi.org/10.1016/j.it.2004.09.015These polarization states reflect the macrophage's ability to adapt and perform specialized roles in immunity and tissue homeostasis.

[18] M. Friedemann *et al.*, "Instructing Human Macrophage Polarization by Stiffness and Glycosaminoglycan Functionalization in 3D Collagen Networks," *Adv. Healthc. Mater.*, vol. 6, no. 7, p. 1600967, Apr. 2017, doi: 10.1002/adhm.201600967.

[19] F. Mei *et al.*, "Matrix stiffness regulates macrophage polarisation via the PIEZO1-YAP signalling axis," *Cell Prolif.*, vol. 57, no. 8, p. e13640, Aug. 2024, doi: 10.1111/cpr.13640.

[20] F. Y. McWhorter, C. T. Davis, and W. F. Liu, "Physical and mechanical regulation of macrophage phenotype and function," *Cell. Mol. Life Sci.*, vol. 72, no. 7, pp. 1303–1316, Apr. 2015, doi: 10.1007/s00018-014-1796-8.

[21] M. L. Previtera and A. Sengupta, "Substrate Stiffness Regulates Proinflammatory Mediator Production through TLR4 Activity in Macrophages," *PLOS ONE*, vol. 10, no. 12, p. e0145813, Dec. 2015, doi: 10.1371/journal.pone.0145813.

[22] R. A. Scott, K. L. Kiick, and R. E. Akins, "Substrate stiffness directs the phenotype and polarization state of cord blood derived macrophages," *Acta Biomater.*, vol. 122, pp. 220–235, Mar. 2021, doi: 10.1016/j.actbio.2020.12.040.

[23] R. Sridharan, B. Cavanagh, A. R. Cameron, D. J. Kelly, and F. J. O'Brien, "Material stiffness influences the polarization state, function and migration mode of macrophages," *Acta Biomater.*, vol. 89, pp. 47–59, Apr. 2019, doi: 10.1016/j.actbio.2019.02.048.

[24] F. Mei *et al.*, "Matrix stiffness regulates macrophage polarisation via the PIEZO1-YAP signalling axis," *Cell Prolif.*, vol. 57, no. 8, p. e13640, Aug. 2024, doi: 10.1111/cpr.13640.

[25] N. Helleberg Madsen, B. Schnack Nielsen, J. Larsen, and M. Gad, "In vitro 2D and 3D cancer models to evaluate compounds that modulate macrophage polarization," *Cell. Immunol.*, vol. 378, p. 104574, Aug. 2022, doi: 10.1016/j.cellimm.2022.104574.

[26] J. A. Mas-Rosario, J. D. Medor, M. I. Jeffway, J. M. Martínez-Montes, and M. E. Farkas, "Murine macrophage-based iNos reporter reveals polarization and reprogramming in the context of breast cancer," *Front. Oncol.*, vol. 13, p. 1151384, Apr. 2023, doi: 10.3389/fonc.2023.1151384.

[27] S. C. Carrara *et al.*, "3D topographies promote macrophage M2d-Subset differentiation," *Mater. Today Bio*, vol. 24, p. 100897, Feb. 2024, doi: 10.1016/j.mtbio.2023.100897.

[28] B. M. Tiemeijer *et al.*, "Probing Single-Cell Macrophage Polarization and Heterogeneity Using Thermo-Reversible Hydrogels in Droplet-Based Microfluidics," *Front. Bioeng. Biotechnol.*, vol. 9, Oct. 2021, doi: 10.3389/fbioe.2021.715408.

[29] J. Graf *et al.*, "Macrophage variance: investigating how macrophage origin influences responses to soluble and physical cues with immortalized vs. primary cells in 2D and 3D culture," *Front. Biomater. Sci.*, vol. 3, May 2024, doi: 10.3389/fbiom.2024.1399448.

[30] S. Bustin and J. Huggett, "qPCR primer design revisited," *Biomol. Detect. Quantif.*, vol. 14, pp. 19–28, Dec. 2017, doi: 10.1016/j.bdq.2017.11.001.

[31] D. M. Gomez Zubieta, M. A. Hamood, R. Beydoun, A. E. Pall, and K. C. Kondapalli, "MicroRNA-135a regulates NHE9 to inhibit proliferation and migration of glioblastoma cells," *Cell Commun. Signal.*, vol. 15, no. 1, p. 55, Dec. 2017, doi: 10.1186/s12964-017-0209-7.

[32] R. A. Scott, K. L. Kiick, and R. E. Akins, "Substrate stiffness directs the phenotype and polarization state of cord blood derived macrophages," *Acta Biomater.*, vol. 122, pp. 220–235, Mar. 2021, doi: 10.1016/j.actbio.2020.12.040.

[33] Mantovani, A., et al. (2013). Macrophage plasticity and polarization in tissue repair and remodeling. Journal of Pathology, 229(2), 176–185. https://doi.org/10.1002/path.4133

[34] Burgess, D. J. (2018). Human tissue models: Bridging the translational gap. Nature Reviews Drug Discovery, 17(12), 845–846. https://doi.org/10.1038/nrd.2018.205

[35] V. J. Thannickal *et al.*, "Matrix Biology of Idiopathic Pulmonary Fibrosis," *Am. J. Pathol.*, vol. 184, no. 6, pp. 1643–1651, Jun. 2014, doi: 10.1016/j.ajpath.2014.02.003.

8. SUPPLEMENTARY MATERIAL

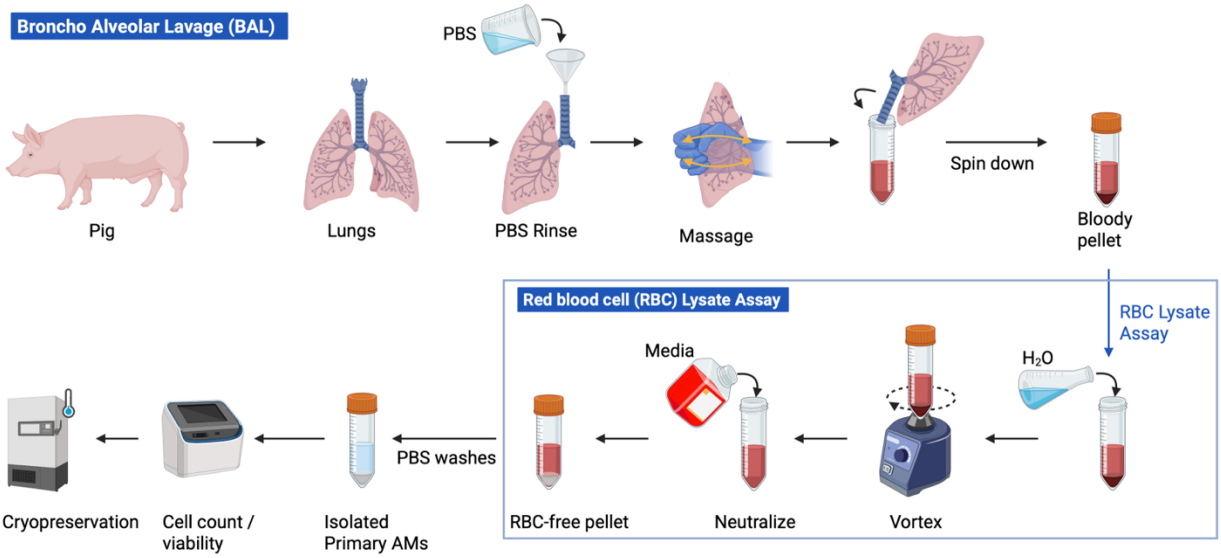


Fig S1: Schematic representation of the procedure used to isolate primary pig AMs via bronchoalveolar lavage. After obtaining the lungs, lobes were washed with sterile PBS through the main bronchus. The lung lobes were massaged to release AMs, and the lavage fluid was collected and centrifuged to obtain a bloody cell pellet. Red blood cells were lysed using a sterile water shock method followed by vortexing, and the solution was neutralized with culture media. The resulting RBC-free cell pellet was washed with PBS, counted for viability, and cryopreserved or used for downstream analyses.

Table S1: Table of forward (F) and reverse (R) primer sequences designed for gene expression analysis of pig-derived AM polarization markers. Genes analyzed include pro-inflammatory (M1-associated) and anti-inflammatory (M2-associated) targets such as IL-1β, IL-6, IL-10, IL-12, IL-23, NOS-1, TNF-α, TGF-β, VEGF, CCL chemokines, and NOX-1. Primer sequences are listed for both mouse and pig species, enabling cross-species comparison in RAW 264.7 murine macrophages and primary porcine alveolar macrophages. Sequences were designed to meet standard qPCR primer design parameters and verified for specificity using NCBI BLAST.

Gene	F / R	Mouse sequence	Pig sequence
IL-1	F	GCAACTGTTCCTGAACTCAACT	CTCTCCAGCCAGTTCTCATTGT
IL-1	R	ATCTTTGGGGTCCGTCAACT	GCTCCCATTTCTCAGAGAAACC
IL-6	F	TAGTCCTTCCTACCCCAATTTCC	TACCAAAGCACTGATGCCAACC
IL-6	R	TTGGTCCTTAGCCACTCCTTC	TCTGTGACTGCAGGATTATCCAG
IL-10	F	ATTTGAATTCCCTGGGTGAGAAG	ACCTTCCAGGATGAGCACTCA
IL-10	R	CACAGGGGAGAAATCGATGACA	TAGTTCACAGAGAGGCTCGGTA
IL-12	F	AGACATCACACGGGACCAAAC	CGTCAGCAACACACTTCAGAAAG
IL-12	R	CCAGGCAACTCTCGTTCTTGT	ATTCTGGCTAGTTCAAGTGGAT
IL-23	F	AATATGACTCAGGGAAGCAGGT	CCTGGACTGCAGATTACCACAT
IL-23	R	GCTCCCTTTGAAGATGCTGAG	CACTGGATATGGGGGACTTCAC
NOS-1	F	CTGGTGAAGGAACGGGTCAG	TATGGAGTGAGACCAGCGAGTA
NOS-1	R	CCGATCATTGACGGCGAGAAT	AAGGTTAGGTCCACAGCTCATG
TNF-α	F	CCTGTAGCCCACGTCGTAG	ACGTTGTAGCCAATGTCAAAGC
TNF-α	R	GGGAGTAGACAAGGTACAACCC	CTGGTGTTCTTTACGCTTCACG
TGF-B	F	CCACCTGCAAGACCATCGAC	AGGAGGATTGAGCCACCAATT
TGF-B	R	CTGCGGACCTATTGTTGGAC	CTGAAGCAGGATTTCAGGAGAGT
CCL-1	F	TGCCTGTGGATACAGAGACTG	GGATTTCCCTGGAAGAGATCCA
CCL-1	R	GTTGAGGCGGACTTTCTCTA	GGGCCTCCGATCAGCTTCAATAT
CCL-17	F	TACCATGAGTCACTTCAGATGC	CATTGTGCTTTGACCTTCCAG
CCL-17	R	GGACTTCGGCTTCTCATGTTTT	GGTCCTGGGCTTCATTGTTTT
CCL-22	F	AGGTCCCATTGGTGCCAATGT	CTGTCCACCTCAGTCAAGTCTC
CCL-22	R	CGGCAGGATTGAGGTCCAC	ATGACTGACCAGGATTGGGAC
CCL-24	F	ATTCTGGTGACTCCCTCCAC	CCTTCTCTGACTTCGGGTTCC
CCL-24	R	TGTATGCTCCTTGAACCCAC	TCACCCAGCAGAGAGACAGACA
VEGF	F	GCAATGAGGGCCCATGC	CGCTTTCAAAGGAGAAAAGC
VEGF	R	CTCCCTCTTGAAGGAGCATG	GGAAATGGAGATCAAGGCTGA
NOX-1	F	GGTTGGGGCATCGTTACC	GACAGGCCTGAAGAAGAAACC
NOX-1	R	TCGAACACACAGGGCTTGA	GGGGTTGAATTGGAGCTGTAGA

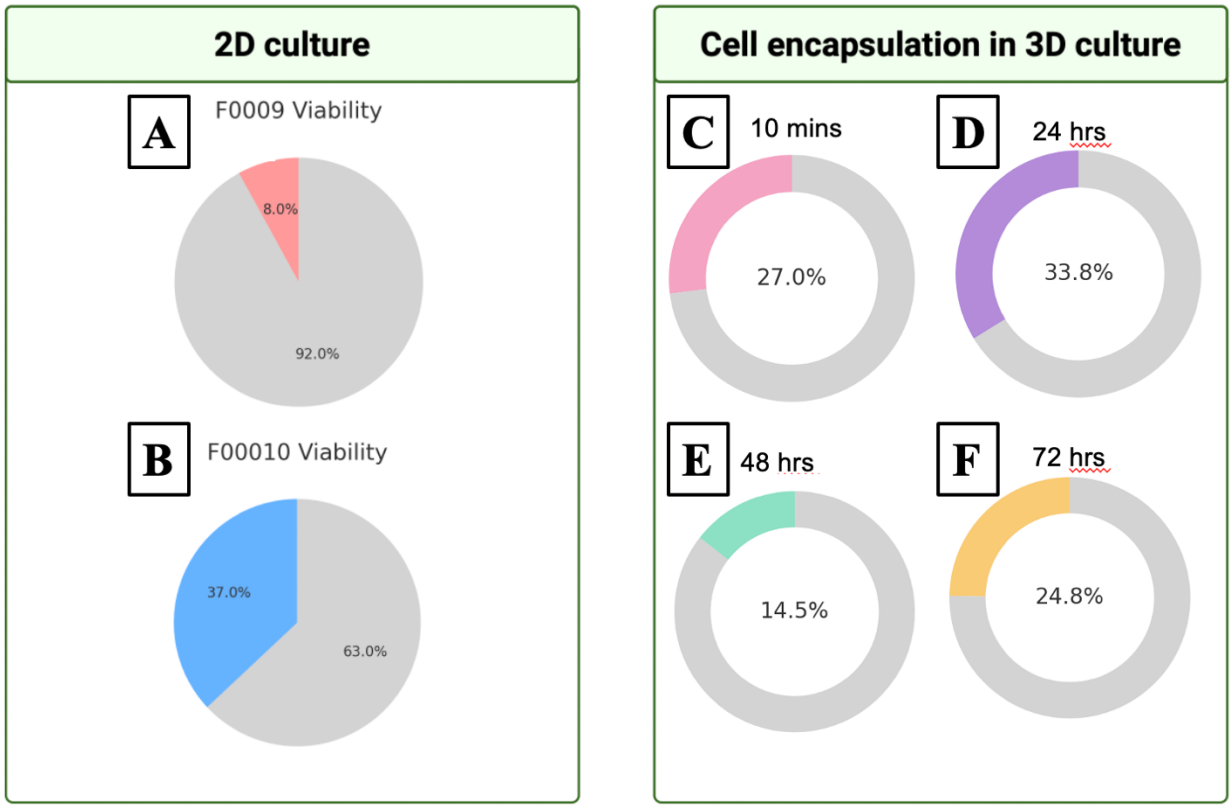


Fig S2: Left panel: viability of AMs derived from two pig lungs (A) from F0009 and (B) from F00010 after being cultured in standard 2D conditions for 7 days. Viability was determined by manual cell counts using the hemocytometer. Right panel: recovery rates of F00010-derived AMs following encapsulation in 3D alginate hydrogels at indicated time points (C) 10 minutes, (D) 24 hours, (E) 48 hours, and (F) 72 hours. Recovery was calculated as the percentage of viable cells recovered relative to the number initially encapsulated.